2016 IEEE Conference on Control Applications (CCA)
Part of 2016 IEEE Multi-Conference on Systems and Control
September 19-22, 2016. Buenos Aires, Argentina

Hybrid Acceleration/Velocity-based Disturbance Observer for a Quadrotor Manipulation System

Ahmed Khalifa[1], Mohamed Fanni[2] and Toru Namerikawa[3]

Abstract— **Aerial manipulation systems become very attractive for a wide range of applications due to their unique features. However, control of such system is quite challenging due to its high nonlinearities, couplings, and external disturbances. In this paper, a Disturbance Observer (DOb)-based linearization of a quadrotor manipulation system is utilized. The DOb estimates the disturbances and nonlinearities, then compensates them such that one can treat the control problem based on a simple linear control algorithm. However, the current developed DOb schemes in the literature are based on the precise measurement of the acceleration or the estimation of the velocity. Unlike, these methods, we propose a modified DOb, which is based on both the measured linear accelerations and angular velocities that can be obtained directly from the onboard Inertial Measurement Unit (IMU) and encoders. With this technique, the estimation of nonlinearities and disturbances are carried out without the need of estimation acceleration or velocity, and it is model free. The Effectiveness of the proposed technique is verified via numerical simulations.**

I. Introduction

Recently, aerial manipulators have much interest because they have several vital applications in the places which are not accessible by ground robots. Due to the superior mobility of quadrotors, they are utilized for mobile manipulation. Such systems open new application area for robotics. Such applications are inspection, maintenance, firefighting, service robot in crowded cities to deliver light stuff such as post mails or quick meals, rescue operation, surveillance, demining, performing tasks in dangerous places, or transportation in remote places.

Several researches have been introduced in the area of aerial manipulation [1]–[5]. However, the previous introduced systems in the literature that use a gripper suffer from the limited allowable DOF of the end-effector. The other systems have a manipulator with either two DOF but in certain topology that disables the end-effector to track arbitrary 6-DOF trajectory, or more than two DOF which decreases greatly the possible payload carried by the system. Moreover, the control schemes that were presented in the literature for such robots are based on nonlinear controllers which are very complicated and have very high computational cost.

One of the key issues for aerial manipulation is achieving the position holding. In order to achieve this task, a robust control must be implemented such that it can cope up with the nonlinearities, couplings, uncertainties, and disturbances. The robustness issue for such system is addressed in [6] by using a DOb based control technique. The DOb estimates the nonlinear terms and uncertainties then compensates them such that the robotic system acts like a multi-SISO linear systems. Therefore, it is possible to rely on the standard linear control methodology to design the controller of the outer loop such that the system performance can be adjusted to meet desired tracking accuracy.

However, the previous work [7]–[13] in the DOb requires the estimation of the acceleration or the velocity of the system that is very difficult to obtain and has limitations due to the available sensor for flying robots. Moreover, it is feasible to measure the linear accelerations and angular velocities via IMU and encoders. In [14], the external wrench is estimated by using a model-based method for a simple UAV. In addition, the author utilizes the IMU data for the estimation. However, this method needs to know the dynamic models, neglects some dynamics and nonlinearities, uses a nonlinear controller, estimates only the external disturbances without estimating the system dynamics. Thus, this technique is not good choice for the considered aerial manipulator which is high complex dynamical and kinematic robotic system.

To cope up with these limitations, the conventional DOb is modified to be compatible and feasible with the aerial manipulation system. Firstly, the conventional DOb is redesigned and reformulated to use the linear acceleration and angular velocities data, which can be measured directly via the onboard IMU and encoders, to estimate the disturbances and nonlinearities. Secondly, this estimated data is fed back to the system such that it can be compensated and the system becomes linear. Thirdly, a performance linear controller is designed in the outer loop to achieve the objective response. Fourthly, a Jacobian based inverse kinematics algorithm is presented such that one can track desired 6-DOF task space trajectories. Finally, a simulation setup, with some non-idealities to emulate a realistic one, is built to verify the proposed technique.

This paper is organized as follows: In section II, the considered robot is described, and kinematic and dynamic analysis are reviewed. The control problem is formulated and presented in section III. In section IV, simulation results

[1]Ahmed Khalifa is with Department of System Design Engineering, Keio University, Yokohama, Japan. On study leave from Department of Mechatronics and Robotics Engineering, Egypt-Japan University of Science and Technology, Alexandria, Egypt. ahmed.khalifa@ejust.edu.eg

[2]Mohamed Fanni is with Department of Mechatronics and Robotics Engineering, Egypt-Japan University of Science and Technology. On leave from Department of Production Engineering and Mechanical Design, Mansoura University, Mansoura, Egypt. mohamed.fanni@ejust.edu.eg

[3]Toru Namerikawa is with Department of System Design Engineering, Keio University, Yokohama, Japan. namerikawa@nl.sd.keio.ac.jp

978-1-5090-0755-4/16/$31.00 ©2016 IEEE

using MATLAB/SIMULINK are presented. Finally, the main contributions are presented in section V.

II. Mathematical Model

Design and modeling of the quadrotor manipulation system are presented in details in [5]. The system consists mainly of two parts; the quadrotor and the manipulator. 3D CAD model of it is shown in Fig. 1. Fig. 2 presents a sketch

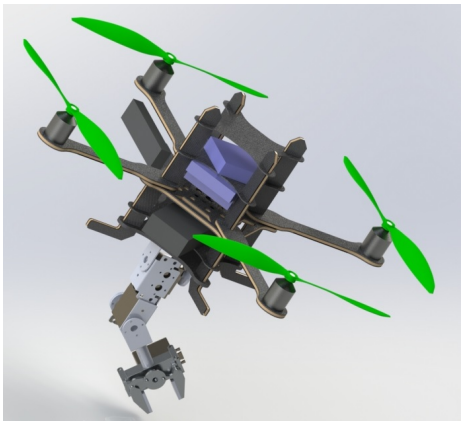

Fig. 1. 3D CAD model of the Quadrotor Manipulation System

of such system with the relevant frames which indicates the unique topology that permits the end-effector to achieve arbitrary pose. The frames satisfy the Denavit-Hartenberg (DH) convention. The quadrotor components are selected

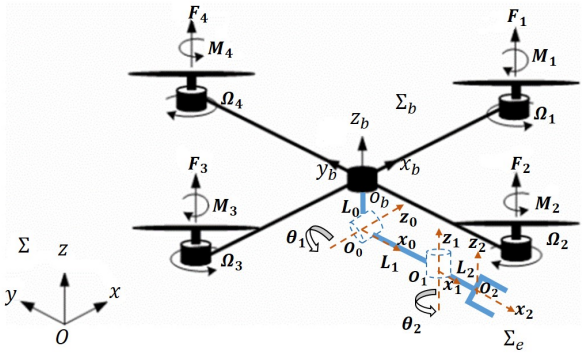

Fig. 2. Schematic diagram of Quadrotor Manipulation System with relevant frames

such that it can carry a payload equals 500 g (larger than the total arm weight and the maximum payload). Asctec pelican quadrotor is used as the quadrotor platform. The maximum thrust force for each rotor is 8 N as obtained from an identification process.

The arm components are designed, selected, purchased and assembled such that the total weight of the arm is 200 g, has maximum reach in the range between 22 cm to 25 cm, and can carry a payload of 200 g. Three DC motors, (HS-422 (Max torque = 0.4 N.m) for gripper, HS-5485HB (Max torque = 0.7 N.m) for joint 1, and HS-422 (Max torque = 0.4 N.m) for joint 2), are used.

Each rotor j has angular velocity Ω_j and it produces thrust force F_j and drag moment M_j which are given by:

$$F_j = K_{f_j}\Omega_j^2, \tag{1}$$

$$M_j = K_{m_j}\Omega_j^2, \tag{2}$$

where K_{f_j} and K_{m_j} are the thrust and drag coefficients.

Let Σ_b, O_b- x_b y_b z_b, denotes the vehicle body-fixed reference frame with origin at the quadrotor center of mass, see Fig. 2. Its position with respect to the world-fixed inertial reference frame, Σ, O- x y z, is given by the (3×1) vector $p_b = [x\ y\ z]^T$, while its orientation is represented by Φ_b=$[\psi\ \theta\ \phi]^T$, and is given by a rotation matrix R_b, which is given by

$$R_b = \begin{bmatrix} C_\psi C_\theta & S_\psi S_\theta C_\psi - S_\psi C_\phi & S_\psi S_\phi + C_\psi S_\theta C_\phi \\ S_\psi C_\theta & C_\psi C_\phi + S_\psi S_\theta S_\phi & S_\psi S_\theta C_\phi - C_\psi S_\phi \\ -S_\theta & C_\theta S_\phi & C_\theta C_\phi \end{bmatrix}, \tag{3}$$

where Φ_b=$[\psi\ \theta\ \phi]^T$ is the triple ZYX yaw-pitch-roll angles. Note that $C_.$ and $S_.$ are short notations for $\cos(.)$ and $\sin(.)$, respectively.

Let us consider the frame Σ_e, O_2- x_2 y_2 z_2, attached to the end-effector of the manipulator, see Fig. 2. Thus, the position of Σ_e with respect to Σ is given by

$$p_e = p_b + R_b p_{eb}^b, \tag{4}$$

where the vector p_{eb}^b describes the position of Σ_e with respect to Σ_b expressed in Σ_b. The orientation of Σ_e can be defined by the rotation matrix

$$R_e = R_b R_e^b, \tag{5}$$

where R_e^b describes the orientation of Σ_e w.r.t Σ_b.

The generalized end-effector velocity, $v_e = [\dot{p}_e^T, \omega_e^T]^T$, can be expressed as

$$v_e = J_b Q_b \dot{\chi}_b + J_{eb}\dot{\Theta}, \tag{6}$$

with $\chi_b = \begin{bmatrix} p_b \\ \Phi_b \end{bmatrix}$, $Q_b = \begin{bmatrix} I_3 & O_3 \\ O_3 & T_b \end{bmatrix}$, where T_b describes the transformation matrix between the angular velocity, ω_b, and the time derivative of Euler angles, $\dot{\Phi}_b$, and it is given as

$$T_b(\Phi_b) = \begin{bmatrix} 0 & -S_\psi & C_\psi C_\theta \\ 0 & C_\psi & S_\psi C_\theta \\ 1 & 0 & -S_\theta \end{bmatrix}. \tag{7}$$

$$J_b = \begin{bmatrix} I_3 & -Skew(R_b p_{eb}^b) \\ O_3 & I_3 \end{bmatrix}, \ J_{eb} = \begin{bmatrix} R_b & O_3 \\ O_3 & R_b \end{bmatrix} J_{eb}^b,$$

I_m and O_m denote $(m \times m)$ identity and $(m \times m)$ null matrices, respectively, and $Skew(.)$ is the (3×3) skew-symmetric matrix operator [15]. $\Theta = [\theta_1, \theta_2]^T$ be the (2×1) vector of joint angles of the manipulator. J_{eb}^b is the manipulator Jacobian [16].

Since the vehicle is an under-actuated system, i.e., only 4 independent control inputs are available for the 6-DOF system, the position and the yaw angle are usually the controlled variables. The pitch and roll angles are used as intermediate control inputs to control the horizontal position.

Hence, it is worth rewriting the vector χ_b as follows $\chi_b = \begin{bmatrix}\eta_b \\ \sigma_b\end{bmatrix}$, $\eta_b = \begin{bmatrix}p_b \\ \psi\end{bmatrix}$, $\sigma_b = \begin{bmatrix}\theta \\ \phi\end{bmatrix}$.

Thus, the differential kinematics (6) will be

$$\begin{aligned} v_e &= J_\eta \dot{\eta}_b + J_\sigma \dot{\sigma}_b + J_{eb}\dot{\Theta} \\ &= J_\zeta \dot{\zeta} + J_\sigma \dot{\sigma}_b, \end{aligned} \tag{8}$$

where $\zeta = [\eta_b^T, \Theta^T]^T$ is the vector of the controlled variables, J_η is composed by the first 4 columns of $J_b Q_b$, J_σ is composed by the last 2 columns of $J_b Q_b$ and $J_\zeta = [J_\eta, J_{eb}]$.

If the end-effector orientation is expressed via a triple of Euler angles, ZYX, Φ_e, the differential kinematics (8) can be rewritten in terms of the vector $\dot{\chi}_e = [\dot{p}_e^T, \dot{\Phi}_e^T]^T$ as

$$\begin{aligned} \dot{\chi}_e &= Q_e^{-1}(\Phi_e) v_e \\ &= Q_e^{-1}(\Phi_e)[J_\zeta \dot{\zeta} + J_\sigma \dot{\sigma}_b], \end{aligned} \tag{9}$$

where Q_e is the same as Q_b but it is a function of Φ_e instead of Φ_b.

The dynamical model of the quadrotor-manipulator system can be written as follows

$$\begin{aligned} M(q)\ddot{q} + C(q,\dot{q})\dot{q} + G(q) + d_{ex} &= \tau, \\ \tau &= Bu, \end{aligned} \tag{10}$$

where $q = [x\ y\ z\ \psi\ \theta\ \phi\ \theta_1\ \theta_2]^T \in R^8$ is the generalized coordinates, $M \in R^{8\times 8}$ represents the symmetric and positive definite inertia matrix of the combined system, $C \in R^{8\times 8}$ is the matrix of Coriolis and centrifugal terms, $G \in R^8$ is the vector of gravity terms, $d_{ex} \in R^8$ is vector of the external disturbances, $\tau \in R^8$ is vector of the generalized input torques/forces, $u = [F_1, F_2, F_3, F_4, \tau_{m_1}, \tau_{m_2}]^T \in R^6$ is vector of the actuators' inputs, $B = HN \in R^{8\times 6}$ is the input matrix which is used to generate the body forces and moments from the actuators' inputs. $N \in R^{8\times 6}$ is given by

$$N = \begin{bmatrix} 0 & 0 & 0 & 0 & 0 & 0 \\ 0 & 0 & 0 & 0 & 0 & 0 \\ 1 & 1 & 1 & 1 & 0 & 0 \\ \gamma_1 & -\gamma_2 & \gamma_3 & -\gamma_4 & 0 & 0 \\ -d & 0 & d & 0 & 0 & 0 \\ 0 & -d & 0 & d & 0 & 0 \\ 0 & 0 & 0 & 0 & 1 & 0 \\ 0 & 0 & 0 & 0 & 0 & 1 \end{bmatrix}, \tag{11}$$

where $\gamma_j = K_{m_j}/K_{f_j}$, and $H \in R^{8\times 8}$ transforms body input forces to be expressed in Σ and is given by

$$H = \begin{bmatrix} R_b & O_3 & O_2 \\ O_3 & T_b^T R_b & O_2 \\ O_{2x3} & O_{2x3} & I_2 \end{bmatrix}. \tag{12}$$

III. Control System Design

A. Control Objectives

We target the design of the control input, τ, in order to satisfy the following objectives:

Control Objective 1: (System Linearization) The system nonlinearities and external disturbances are estimated by using the measurement data that can be obtained directly form the onboard sensors (i.e., the estimation error, $\tilde{\tau}^{dis}$ = τ^{dis} - $\hat{\tau}^{dis}$, tends to zero as time tends to ∞).

Control Objective 2: (Robust Stability) The considered robotic system is stable and robust against the effects of external disturbances, uncertainties, and measurement noises.

Control Objective 3: (Trajectory Tracking) The end-effector pose error tends to zero as time tends to ∞.

To achieve these control objectives, we propose a control technique based on a modified DOb. In this strategy, the system nonlinearities, uncertainties, external disturbances, τ^{dis}, are treated as disturbances which will be estimated by using the linear accelerations and angular velocities measurements, $\hat{\tau}^{dis}$, and canceled by the DOb in the inner loop. The system can be now considered as linear SISO plants, and thus, the PD loop is used in the external loop to achieved the target performance for the system by producing τ^{des}. The final loop is presented to find the desired quadrotor/joint space trajectories from the target 6-DOF task space. Hence, the controller can be designed in the quadrotor/joint space.

B. DOb Loop

A block diagram of the DOb controller is shown in Fig. 3 which will be utilized later to design robust control for the proposed system. It is well known that the linear accelerations and angular rates of the quadrotor can be measured directly from the IMU. In addition, the angular velocities of the joints can be measured via an encoder. Therefore, two different DOb loops are used. One is based on the measured acceleration, while the other is based on the measured velocity.

In this figure, $M_n = \begin{bmatrix} M_{n_a} & O_{3\times 5} \\ O_{5\times 3} & M_{n_v} \end{bmatrix} \in R^{8\times 8}$ is the system nominal inertia matrix with $M_{n_a} \in R^{3\times 3}$ represents the nominal inertia for accelerations, $\ddot{p}_b$, while $M_{n_v} \in R^{5\times 5}$ represents the nominal inertia for velocities, $\dot{\Phi}_b$ and $\dot{\Theta}$. τ and τ^{des} are the robot and desired inputs, respectively. $Q(s) = diag([\frac{g_1}{s+g_1} \ \ldots \ \frac{g_i}{s+g_i} \ \ldots \ \frac{g_8}{s+g_8}]) \in R^{8\times 8}$ is the matrix of the low pass filter of DOb, $Q_a(s) = diag([\frac{g_1}{s+g_1} \ \ldots \ \frac{g_3}{s+g_3}])$, and $Q_v(s) = diag([\frac{g_4}{s+g_4} \ \ldots \ \frac{g_8}{s+g_8}])$. $P = diag([g_1 \ \ldots \ g_i \ \ldots \ g_8])$ with g_i is the bandwidth of the i^{th} variable of q, and $P_v = diag([g_4 \ \ldots \ g_i \ \ldots \ g_8])$ for the velocity part. τ^{dis} represents the system disturbances including the Coriolis, centrifugal and gravitational terms. $\hat{\tau}^{dis} = [\hat{\tau}_a^{dis^T} \ \hat{\tau}_v^{dis^T}]^T$

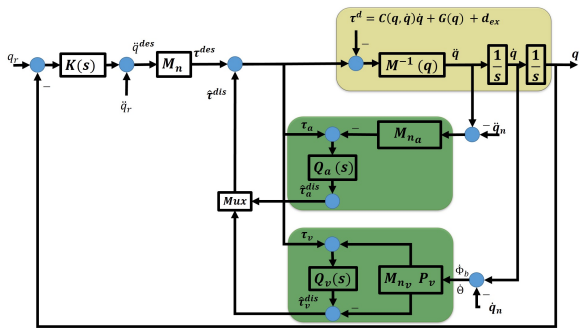

Fig. 3. Block diagram of DOb-based controller

represents the system estimated disturbances.

The system disturbance, τ^{dis}, can be assumed as

$$\begin{aligned} \tau^{dis} &= (M(q) - M_n)\ddot{q} + \tau^d, \\ \tau^d &= C(q,\dot{q})\dot{q} + G(q) + d_{ex}. \end{aligned} \tag{13}$$

The control input, τ, in Fig. 3 can be calculated as

$$\tau = M_n \ddot{q}^{des} + \hat{\tau}^{dis}, \tag{14}$$

where

$$\hat{\tau}^{dis} = Q(\tau - M_n \ddot{q}). \tag{15}$$

This control law leads to the following error dynamics

$$\begin{aligned} M(q)\dot{e}_v + C(q,\dot{q})e_v + K_v e_v = \delta, \\ K_v = PM_n, \end{aligned} \tag{16}$$

where $e_v = \dot{q}^{des} - \dot{q}$, and

$$\delta = \Delta M(q)\ddot{q}^{des} + C(q,\dot{q})\dot{q}^{des} + G(q) + d_{ex}, \tag{17}$$

and $\Delta M(q) = M(q) - M_n$.

Equation (16) represents the error dynamics of the DOb loop. stability of these error dynamics is presented in [6].

If the DOb performs ideally, then on can assume that all the internal and external disturbances are estimated and compensated (i.e. $\hat{\tau}^{dis} = \tau^{dis}$)

Thus, the dynamics from the DOb loop input τ^{des} to the output of the robot manipulator is given by

$$M_n \ddot{q} = \tau^{des}. \tag{18}$$

Since M_n is a diagonal matrix, the system can be treated as multi-decoupled linear SISO systems as

$$M_{n_{ii}} \ddot{q}_i = \tau_i^{des}, \tag{19}$$

or simply in the acceleration space as

$$\ddot{q}_i = \ddot{q}_i^{des}. \tag{20}$$

All that remains in the design of the DOb based controller is the design of the tracking controller, $K(s)$, in the DOb outer loop. A PD-based tracking controller for the system of (20) is chosen as

$$\ddot{q}^{des} = \ddot{q}_r + K_P(q_r - q) + K_D(\dot{q}_r - \dot{q}), \tag{21}$$

where K_P and $K_D \in R^{8\times 8}$ are the proportional and derivative gains of the PD controllers, receptively. q_r, $\dot{q}_r$, and $\ddot{q}_r$ are the references for linear/angular positions, velocities, and accelerations, respectively.

This will lead to the following error dynamics

$$\ddot{e} + K_D\dot{e} + K_P e = 0, \tag{22}$$

where $e = q_r - q$, which are asymptotically stable provided that the gains, K_P and K_D , are positive definite matrices.

C. Jacobian-based Inverse Kinematics

To achieve task space control, the desired 6-DOF trajectories of the end-effector pose, $\chi_{e,r}$, are used to generate the desired trajectories for the quadrotor/joint space independent coordinates, ζ, using the inverse kinematics, while the dependent coordinates, σ_b, can be obtained from the nonholonomic constraints.

The differential kinematics (9) are considered to derive a closed-loop inverse kinematics algorithm [17].

$$\dot{\zeta}_r = J_\zeta^{-1}\{Q_e[\dot{\chi}_{e,r} + K_e e_e] - J_\sigma \dot{\sigma}_b\} \tag{23}$$

where $\dot{\chi}_{e,r}$ is the desired translational and rotational velocities of end-effector, and $e_e = \chi_{e,r} - \chi_e$ is the kinematic inversion error. K_e is a positive definite gain matrix. By integrating, $\dot{\zeta}_r$, one can obtain the desired trajectories in the quadrotor/joint space, ζ_r. The drift of the due to the integration is corrected by the task space error,e_e.

Fig. 4 presents a block diagram of the proposed motion control system based on the inverse kinematics analysis and on quadrotor/joint space-based control. The desired trajectories for the end-effector's position and orientation $\chi_{e,r}$ ($p_{e,r}(t)$ and $\Phi_{e,r}(t)$) are fed to the inverse kinematics algorithm together with $\sigma_{b,r}(t)$ from a simplified version of the nonholonomic constraints such that the desired vehicle/joint space trajectories $\zeta_r(t)$ are obtained. After that, the controller block receives the desired trajectories and the feedback signals from the system and provides the control signal, $\tau = Bu$.

Since the position and the yaw angle are usually the controlled variables while pitch and roll angles are used as intermediate control inputs for horizontal positions control, the proposed control system consists from two DOb-based controllers; one for ζ (with $K_\zeta(s)$, M_{n_a}, M_{nv_1} ,P_{v_1}, Q_{v_1}, and Q_a) and the other for σ_b (with $K_\sigma(s)$, M_{nv_2}, P_{v_2}, Q_{v_2}).

The desired values $\sigma_{b,r}$ for the intermediate controller are obtained from the output of position controller, τ_ζ, through the simplified nonholonomic constraints

$$\sigma_{b,r} = \frac{1}{\tau_\zeta(3)} \begin{bmatrix} C_\psi & S_\psi \\ S_\psi & -C_\psi \end{bmatrix} \begin{bmatrix} \tau_\zeta(1) \\ \tau_\zeta(2) \end{bmatrix} \tag{24}$$

The output of two the controllers, τ_ζ and τ_σ, are mixed to generate the final control vector τ which is converted to the

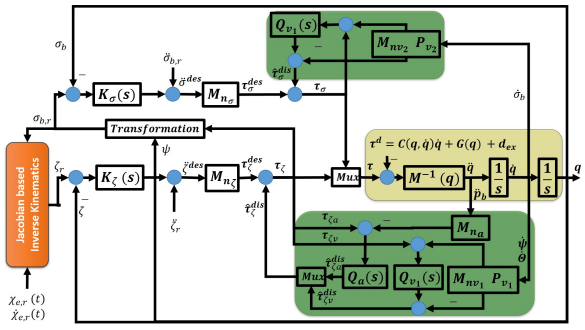

Fig. 4. Detailed block diagram of the control system

TABLE I

DOb BASED CONTROLLER PARAMETERS

Par.	Value	Par.	Value
M_{n_ζ}	$diag\{2\ 2\ 2\ 0.5\ 0.5\ 0.5\}$	M_{n_σ}	$diag\{0.5\ 0.5\}$
K_{P_ζ}	$diag\{3\ 3\ 10\ 3\ 3\ 3\}$	K_{P_σ}	$diag\{10\ 10\}$
K_{D_ζ}	$diag\{1.5\ 1.5\ 5\ 3\ 3\ 3\}$	K_{D_σ}	$diag\{7\ 7\}$
K_e	$diag\{10\ 10\ 10\ 3\ 3\ 3\}$	P	$[10\ 10\ 10\ 100\ 100\ 100\ 100\ 100]^T$

forces/torques applied to quadrotor/manipulator through the following relation:

$$u = B_6^{-1} \begin{bmatrix} \tau_\zeta(3,4) \\ \tau_\sigma \\ \tau_\zeta(5,6) \end{bmatrix}, \tag{25}$$

where $B_6 \in R^{6\times 6}$ is part of B matrix and it is given by $B_6 = B(3:8, 1:6)$.

IV. Simulation Study

In this section, the previously proposed control strategy is simulated in MATLAB/SIMULINK program for the considered aerial manipulation system.

A. Simulation Environment

In order to make the simulation quite realistic, the following setup and assumptions have been made:

- The model has been identified on the basis of real data through experimental tests [18].
- Linear and angular position and velocity of the quadrotor are available at rate of 1 KHz.
- The position and velocity of the manipulator joints are available at rate of 1 KHz [19].
- A normally distributed measurement noise, with mean of 10^{-3} and standard deviation of 5×10^{-3}, has been added to the measured signals.
- The controller outputs are computed at a rate of 1 KHz.
- In order to test the robustness to the model uncertainties, a step disturbance is introduced, at instant 15 s, in the control matrix, N, (Actuators' losses), whose elements are assumed to be equal to 0.9 times their true values (i.e., 10% error).
- The end-effector has to pick a payload of value 200 g at instant 20 g and release it at 40 s.

B. Results and Discussion

Tables I presents the controller parameter for the proposed control technique. The reference trajectories for the end-effector are chosen such that the end-effector moves on a circular helix, while its orientation is fixed in a case and follows quintic polynomial trajectories in another case.

Fig. 5 presents the norm of the estimation error, $\tilde{\tau}^{dis}$, in all coordinates. At the beginning of operation, the error has high value which decreases gradually after about 3 s till reaches to 0. It is noted also that at instants of applying/releasing the payload their is a small error that the DOb recovers it quickly in about 1 s after which the error returns again to 0.

Figs. 6 and 7 show the response of system in the task space (the actual end-effector position and orientation can be found from the forward kinematics). These figures appear the capability of the proposed scheme to track the desired 6-DOF end-effector trajectories in the presence of quite realistic operation non-idealities such as payload handling and measurement noise. Therefore, one can contend that the proposed motion control scheme is able to achieve the control objectives.

V. Conclusion

The issue of a more reliable and efficient robust linearization and control of an aerial manipulation robot is investigated. A modified DOb loop is used to enforce robust linear input/output behavior of the plant by canceling the effect of disturbances, measurement noise, and plant/model mismatch. Unlike the current introduced schemes, the DOb utilizes the available measurement data from the IMU and encoders to estimate the disturbances. After that, the PD controller is used in the external loop to achieve the required closed loop performance and control objectives with low computational load. The system is simulated using MATLAB/SIMULINK. Simulation results enlighten the efficacy of the proposed controller.

Acknowledgment

The first author is supported by a scholarship from the Mission Department, Ministry of Higher Education of the Government of Egypt which is gratefully acknowledged.

References

[1] D. Mellinger, Q. Lindsey, M. Shomin, and V. Kumar, "Design, modeling, estimation and control for aerial grasping and manipulation," in *2011 IEEE/RSJ International Conference on Intelligent Robots and Systems (IROS)*. IEEE, 2011, pp. 2668–2673.

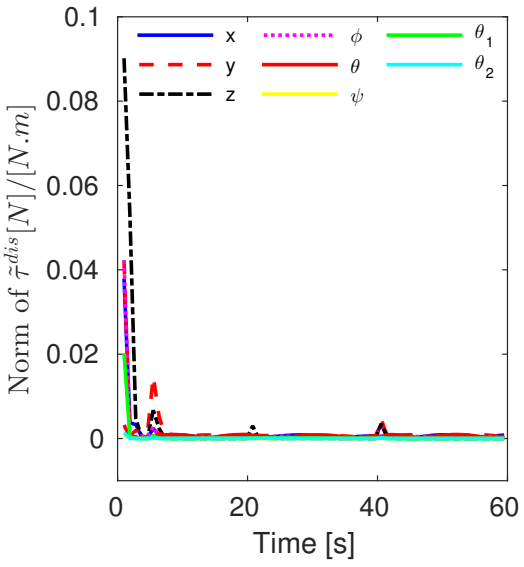

Fig. 5. Norm of the disturbance estimation error

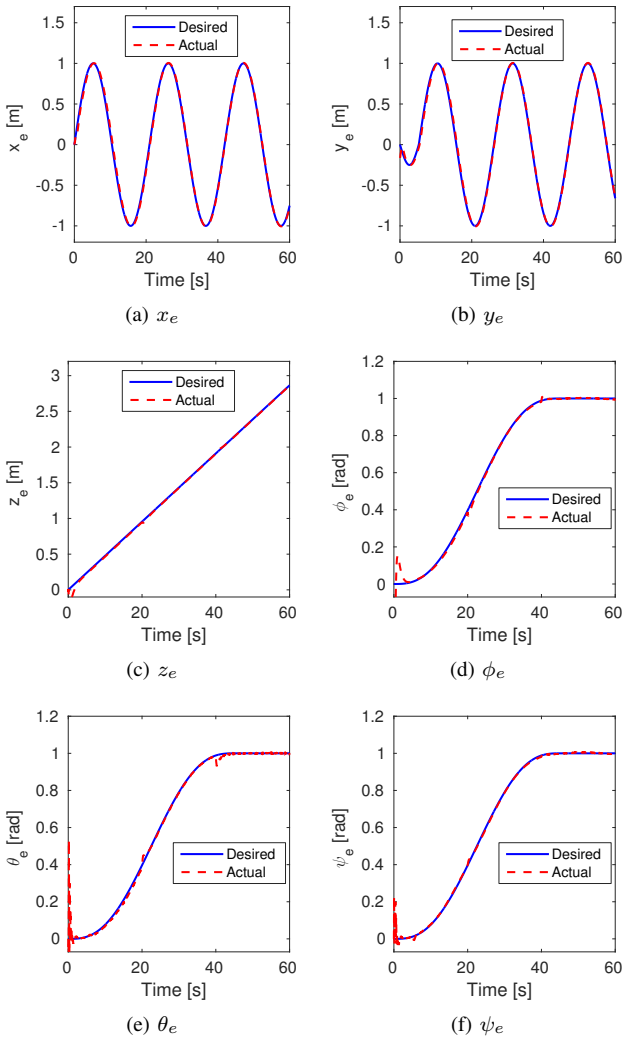

(a) x_e (b) y_e

(c) z_e (d) ϕ_e

(e) θ_e (f) ψ_e

Fig. 6. The actual response of the end-effector position and orientation: a) x_e, b) y_e, c) z_e, d) ϕ_e, e) θ_e, and f) ψ_e

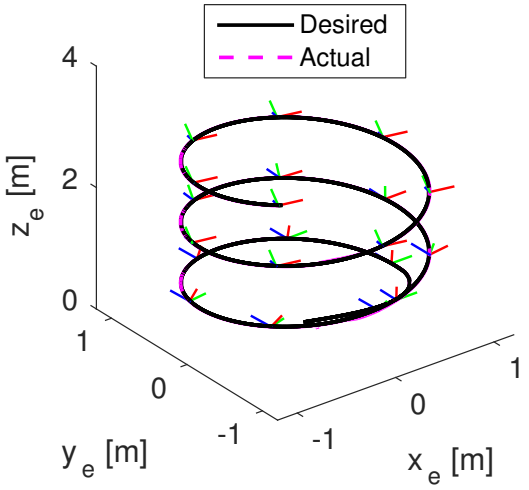

Fig. 7. 3D trajectory of end-effector with fixed orientation (The marker represents the end-effector orientation; Green, Blue, and Red for x-,y, and z-axis)

[2] N. Michael, J. Fink, and V. Kumar, "Cooperative manipulation and transportation with aerial robots," *Autonomous Robots*, vol. 30, no. 1, pp. 73–86, 2011.

[3] C. M. Korpela, T. W. Danko, and P. Y. Oh, "Mm-uav: Mobile manipulating unmanned aerial vehicle," *Journal of Intelligent & Robotic Systems*, vol. 65, no. 1-4, pp. 93–101, 2012.

[4] G. Heredia, A. Jimenez-Cano, I. Sanchez, D. Llorente, V. Vega, J. Braga, J. Acosta, and A. Ollero, "Control of a multirotor outdoor aerial manipulator," in *Intelligent Robots and Systems (IROS 2014), 2014 IEEE/RSJ International Conference on*. IEEE, 2014, pp. 3417–3422.

[5] A. Khalifa, M. Fanni, A. Ramadan, and A. Abo-Ismail, "Modeling and control of a new quadrotor manipulation system," in *2012 IEEE/RAS International Conference on Innovative Engineering Systems*. IEEE, 2012, pp. 109–114.

[6] A. Khalifa, M. Fanni, and T. Namerikawa, "MPC and DOb-based robust optimal control of a new quadrotor manipulation system," in *European Control Conference, Aalborg, Denmark*, June 29 - July 1, 2016, pp. 483 – 488.

[7] B. K. Kim and W. K. Chung, "Performance tuning of robust motion controllers for high-accuracy positioning systems," *Mechatronics, IEEE/ASME Transactions on*, vol. 7, no. 4, pp. 500–514, 2002.

[8] S. Li, J. Yang, W.-h. Chen, and X. Chen, *Disturbance observer-based control: methods and applications*. CRC Press, 2014.

[9] E. Sariyildiz, H. Yu, K. Yu, and K. Ohnishi, "A nonlinear stability analysis for the robust position control problem of robot manipulators via disturbance observer," in *Mechatronics (ICM), 2015 IEEE International Conference on*. IEEE, 2015, pp. 28–33.

[10] K. S. Eom, I. H. Suh, and W. K. Chung, "Disturbance observer based path tracking control of robot manipulator considering torque saturation," *Mechatronics*, vol. 11, no. 3, pp. 325–343, 2001.

[11] H.-T. Choi, S. Kim, J. Choi, Y. Lee, T.-J. Kim, and J.-W. Lee, "A simplified model based disturbance rejection control for highly accurate positioning of an underwater robot," in *Oceans-St. John's, 2014*. IEEE, 2014, pp. 1–5.

[12] T. Hsia, T. Lasky, and Z. Guo, "Robust independent robot joint control: design and experimentation," in *Robotics and Automation, 1988. Proceedings., 1988 IEEE International Conference on*. IEEE, 1988, pp. 1329–1334.

[13] E. Sariyildiz and K. Ohnishi, "Stability and robustness of disturbance-observer-based motion control systems," *Industrial Electronics, IEEE Transactions on*, vol. 62, no. 1, pp. 414–422, 2015.

[14] T. Tomic and S. Haddadin, "A unified framework for external wrench estimation, interaction control and collision reflexes for flying robots," in *Intelligent Robots and Systems (IROS 2014), 2014 IEEE/RSJ International Conference on*. IEEE, 2014, pp. 4197–4204.

[15] M. W. Spong, S. Hutchinson, and M. Vidyasagar, *Robot modeling and control*. Wiley New York, 2006, vol. 3.

[16] L.-W. Tsai, *Robot analysis: the mechanics of serial and parallel manipulators*. Wiley-Interscience, 1999.

[17] B. Siciliano, L. Sciavicco, L. Villani, and G. Oriolo, *Robotics: modelling, planning and control*. Springer Science & Business Media, 2009.

[18] A. Khalifa and M. Fanni, "Position inverse kinematics and robust internal-loop compensator-based control of a new quadrotor manipulation system," *International Journal of Imaging and Robotics*, vol. 16, no. 1, pp. 94–113, 2016.

[19] M. Achtelik, M. Achtelik, S. Weiss, and R. Siegwart, "Onboard imu and monocular vision based control for mavs in unknown in-and outdoor environments," in *Robotics and automation (ICRA), 2011 IEEE international conference on*. IEEE, 2011, pp. 3056–3063.